Int J Cardiovasc Imaging (2015) 31:1663–1675
DOI 10.1007/s10554-015-0750-7

ORIGINAL PAPER

Computed tomography segmental calcium score (SCS) to predict stenosis severity of calcified coronary lesions

Francesca Pugliese[1] · M. G. M. Hunink[2,3] · Willem B. Meijboom[4] · Katarzyna Gruszczynsnka[5] · Marco Rengo[6] · Lu Zou[7] · Ian Baron[5] · Marcel L. Dijkshoorn[2] · Gabriel P. Krestin[2] · Pim J. de Feyter[2,4]

Received: 31 March 2015 / Accepted: 29 July 2015 / Published online: 14 September 2015

Abstract To estimate the probability of ≥50 % coronary stenoses based on computed tomography (CT) segmental calcium score (SCS) and clinical factors. The Institutional Review Board approved the study. A training sample of 201 patients underwent CT calcium scoring and conventional coronary angiography (CCA). All patients consented to undergo CT before CCA after being informed of the additional radiation dose. SCS and calcification morphology were assessed in individual coronary segments. We explored the predictive value of patient's symptoms, clinical history, SCS and calcification morphology. We developed a prediction model in the training sample based on these variables then tested it in an independent test sample. The odds ratio (OR) for ≥50 % coronary stenosis was 1.8-fold greater ($p = 0.006$) in patients with typical chest pain, twofold ($p = 0.014$) greater in patients with acute coronary syndromes, twofold greater ($p < 0.001$) in patients with prior myocardial infarction. Spotty calcifications had an OR for ≥50 % stenosis 2.3-fold ($p < 0.001$) greater than the absence of calcifications, wide calcifications 2.7-fold ($p < 0.001$) greater, diffuse calcifications 4.6-fold ($p < 0.001$) greater. In middle segments, each unit of SCS had an OR 1.2-fold ($p < 0.001$) greater than in distal segments; in proximal segments the OR was 1.1-fold greater ($p = 0.021$). The ROC curve area of the prediction model was 0.795 (0.95 confidence interval 0.602–0.843). Validation in a test sample of 201 independent patients showed consistent diagnostic performance. In conjunction with calcification morphology, anatomical location, patient's symptoms and clinical history, SCS can be helpful to estimate the probability of ≥50 % coronary stenosis.

✉ Francesca Pugliese
f.pugliese@qmul.ac.uk

[1] Centre for Advanced Cardiovascular Imaging, NIHR Cardiovascular Biomedical Research Unit at Barts, William Harvey Research Institute, Barts and The London School of Medicine and Dentistry, Queen Mary University of London, London, UK

[2] Department of Radiology, Erasmus MC University Medical Centre Rotterdam, Rotterdam, The Netherlands

[3] Harvard School of Public Health, Harvard University, Boston, MA, USA

[4] Department of Cardiology, Erasmus MC University Medical Centre Rotterdam, Rotterdam, The Netherlands

[5] Medical University of Silesia, Katowice, Poland

[6] University of Rome La Sapienza, Polo Pontino, Italy

[7] Experimental Medicine and Rheumatology, William Harvey Research Institute, Barts and The London School of Medicine and Dentistry, Queen Mary University of London, London, UK

Keywords Computed tomography · Coronary computed tomography angiography · Coronary calcification · Atherosclerosis · Coronary arteries

Abbreviations

CT	Computed tomography
SCS	Segmental calcium score
CCTA	Coronary computed tomography angiography
CCA	Conventional coronary angiography
OR	Odds ratio
CI	Confidence interval
ROC	Receiver operating characteristic
AUC	Area under the curve
EBT	Electron-beam tomography

Bpm	Beats per minute
ECG	Electrocardiogram
AHA	American Heart Association
QCA	Quantitative coronary angiography
RCA	Right coronary artery
LAD	Left anterior descending coronary artery
LCx	Left circumflex artery
LM	Left main trunk

Introduction

The total amount of coronary artery calcification quantified by electron beam tomography or more recently by multidetector computed tomography (CT) correlates with the probability of angiographically significant (≥50 % diameter reduction) stenosis at the patient level [1–4]. A calcium score of 0 indicates a low probability of ≥50 % coronary stenosis [1]. A calcium score ≥400 indicates a relatively high probability of ≥50 % coronary stenosis in patients ≥50 years old anywhere in the coronary tree. This information is not site-specific. The total calcium score does not provide information regarding the probability of stenosis at the level of a specific coronary segment or lesion. Moreover, the relationship between intermediate values of calcium score (e.g., between 1 and 399) and associated stenosis is weak. Contrast-enhanced coronary CT angiography (CCTA) can overcome the known diagnostic limitations of calcium score. Unfortunately though, bulky calcifications may hinder the visualization of the coronary lumen at CCTA ("blooming effect"), thus the evaluation of stenosis severity in calcified vessels can be challenging.

The purpose of this study was to develop an algorithm for estimating the probability ≥50 % coronary stenoses based on CT segmental calcium score (SCS) and clinical factors. The algorithm consists of a multivariable prediction model that includes the SCS measured in a given coronary segment, the patient's symptoms and clinical history to calculate the probability of ≥50 % coronary artery stenosis in the same coronary segment.

Materials and methods

Patients

The Institutional Review Board approved the study protocol. All patients consented to undergo CT before CCA after being informed of the additional radiation dose. They also consented on the use of their data for retrospective research.

During a 24-month period, 402 patients with stable or acute chest pain were recruited to an ongoing study [5] comparing 64-detector row CCTA with conventional coronary angiography (CCA). Patients in sinus heart rhythm, able to hold their breath for 15 s and without previous coronary revascularization were included. Impaired renal function (serum creatinine >120 μmol/L) and known contrast allergy were exclusion criteria.

Preparation and coronary calcium scans

Patients with heart rates >65 beats per minute (bpm) received 100 mg metoprolol orally 1 h before the scan. Scans were performed with a 64-detector row CT scanner with a gantry rotation time of 330 ms, a temporal resolution of 165 ms and a spatial resolution of 0.4 mm^3 (Somatom Sensation 64; Siemens, Forchheim, Erlangen, Germany).

The non-enhanced coronary calcium scans were acquired with a standard spiral low-dose protocol using ECG-gating. Scan parameters were as follows: 32 × 2 slices per rotation with z-flying focal spot technology, providing 64 slices/rotation; 0.6 mm individual detector width, 330 ms rotation time, 3.8 mm/rotation table feed, 19.2 mm beam width, 11.5 mm/s table speed, 120 kV tube voltage, 150 mAs tube current, with activated prospective X-ray tube modulation. Overlapping slices were reconstructed at 65 % of the R–R interval (retrospective ECG-gating) using B35f convolution kernel. Reconstructed slice thickness was 3.0 mm with an increment of 1.5 mm. The radiation exposure, estimated using dedicated software (ImPACT, version 0.99x, St. George's Hospital, Tooting, London, United Kingdom), was 1.4 mSv in men and 1.8 mSv in women.

Computed tomography coronary angiography (CCTA) scans

For the contrast-enhanced CCTA studies, 80 mL of contrast agent (iomeprol; Iomeron, 400 mg/mL; Bracco, Milan, Italy) were injected intravenously into an antecubital vein. The injection rate was 5 mL/s. A bolus-tracking technique was used to time the scan [5–7]. Scan parameters were identical to those used for coronary calcium scanning except for a tube current of 900 mAs. Datasets were reconstructed using retrospective ECG gating and a monosegmental reconstruction algorithm [5–7]. Overlapping slices were reconstructed at 65 % of the R–R interval (retrospective ECG-gating) using a medium-smooth convolution kernel. Reconstructed slice thickness was 0.75 mm with an increment of 0.4 mm. The estimated

radiation exposure was 14.2 mSv in men and 18.4 mSv in women, in keeping with estimated X-ray radiation exposure values reported using similar CT technology (64-slice) and scan protocol (retrospective ECG-gating) [8].

Conventional coronary angiography (CCA)

CT and CCA were carried out within a time interval of 1 week. A single observer (>10-year experience) identified coronary segments on CCA following a 17-segment modified American Heart Association (AHA) classification model [9]. Coronary stenoses with diameter reduction ≥50 % were identified using validated quantitative coronary angiography (QCA) software (CAAS II®, Pie Medical, Maastricht, the Netherlands).

Analysis of segmental calcium score (SCS) and calcification morphology

CT datasets were analyzed using an off-line workstation (syngo MultiModality Workplace VE25A, Siemens, Erlangen, Germany). Dedicated software (syngo Calcium Scoring VE31H, Siemens, Germany) was used for measuring calcium score in non-enhanced scans [10]. One experienced observer, unaware of the CCA results, measured SCS in individual coronary segments using a standard technique based on seed points and a region-growing algorithm. Results were expressed using the Agatston [11], volume [12] and mass [13] scores. The analysis is described in detail in Figs. 1 and 2. As shown in Fig. 3, calcification morphology in each segment was classified as spotty, wide or diffuse based on the width and length of the calcification in relation to the coronary segment diameter, following a validated classification model previously described by Kajinami et al. [14] (Table 1). In the event of multiple calcifications with different morphology within the same segment, the segment was classified as the calcification with the largest size.

In this study the outcome of interest was ≥50 % diameter stenosis as demonstrated by the gold standard invasive CCA. CCTA was used exclusively for the anatomical classification of coronary segments, but not for grading lesion severity. The evaluation of the diagnostic performance of CCTA in the identification of coronary stenosis compared to CCA was reported previously [6] and was beyond the purpose of this study.

Statistical analysis

Statistical analysis was performed using commercially available software (IBM SPSS, version 20, Chicago, IL, and STATA/SE 10.0, College Station, TX). Quantitative variables were expressed as means (standard deviations) and categorical variables were expressed as frequencies or percentages. The definitions of variables such as symptoms and risk factors are given in Table 2. The level of significance was chosen at a p value <0.05.

Data from 402 patients were split into two equal-sized datasets. One dataset containing 201 patients was used to derive the multivariable prediction model (training set) and the remaining 201 patients were used to validate the prediction model (test set). Baseline characteristics were compared between two sets (Table 2). Continuous variables were tested using Mann–Whitney U test and categorical variables were compared with the Chi squared statistic.

In the training set, we identified highly correlated variables, explored the predictive value of the variables and derived a multivariable prediction model. There was high correlation between the Agatston and the volume scores (Pearson $r = 0.990$; $p < 0.001$), the Agatston and the mass scores ($r = 0.995$; $p < 0.001$) and the volume and the mass scores ($r = 0.989$; $p < 0.001$). We used the Agatston score for further analyses because it has been extensively validated in clinical practice [1–4, 11]. In the training set, we determined the frequency of the outcome of interest i.e., ≥50 % stenoses at the segment level according to ranges of SCS and calcification morphology. Stenoses with a diameter narrowing ≥50 % at CCA were defined as the reference standard to define positive cases. This is in accordance to the definition of 'significant' stenosis most widely used in cardiac CT literature. The natural log transforms of (SCS + 1) were used because SCS showed a skewed distribution.

We performed univariable analyses to evaluate the significance of SCS in each segment, calcification morphology, segment location (proximal, middle, and distal/side branches, as previously described [15]), major coronary vessel (RCA, LAD, LCx, LM), age, gender, patient's symptoms (typical chest pain/atypical chest pain/acute coronary syndrome), risk factors (obesity, hypertension, smoking, diabetes mellitus, hypercholesterolemia, family history of premature coronary artery disease) and clinical history (prior myocardial infarction) for the prediction of ≥50 % stenosis. Variables with a p value <0.10 in the univariable analyses were entered in the multivariable model. Interaction terms were explored between morphology and SCS, location and SCS, location and morphology, vessel and SCS, and vessel and morphology. The final multivariable model included all variables with a p value <0.05 and variables with a p value <0.10 that were considered to be important based on clinical judgment and internal consistency of the model. Odds ratios (OR) and robust 95 % confidence intervals (CI) are reported.

Generalized estimating equations (GEE) with binomial family logit link function, exchangeable correlation matrix, and robust—sandwich—standard errors was applied to drive

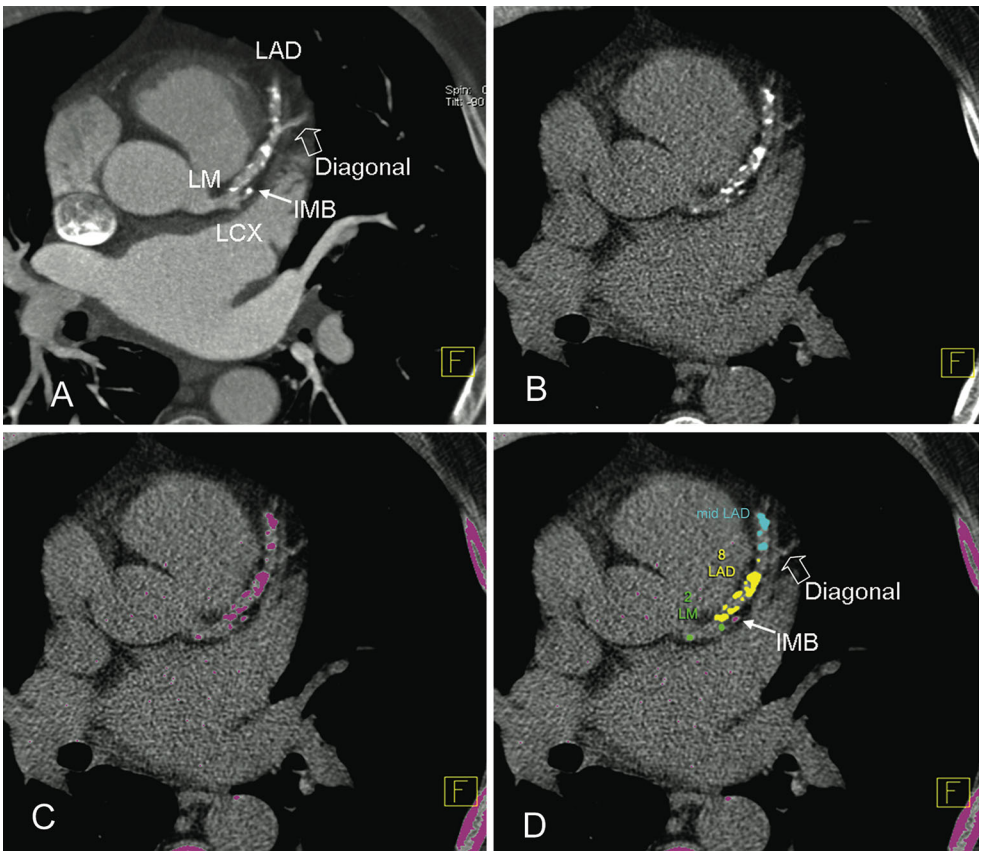

Fig. 1 Method for the measurement of SCS. In order to obtain a consistent anatomic classification of the coronary tree into segments, contrast-enhanced CCTA axial images (**a**) were available to the observer. The CCTA images were scrolled using a viewing application (syngo Viewing, Siemens, Erlangen, Germany). Availability of CCTA ensured the visualization of the origin of smaller side branches, especially when they were not calcified. These side branches might have remained undetected on the non-enhanced images (**b**, **c**). The visualization of the diagonal branches allowed the classification into segments of the left anterior descending coronary artery (LAD); the origin of marginal obtuse branches allowed the classification into segments of the left circumflex artery (LCx), and the origin of acute marginal branches allowed the classification into segments of the right coronary artery (RCA). CCTA was used exclusively for the correct anatomical classification of coronary segments and not for SCS measurement or estimation of stenosis severity. SCS was measured on non-enhanced images [42]. Individual coronary segments were labelled according to a standard 17-segment anatomical (**d**). *LM* left main artery, *LAD* left anterior descending artery, *LCx* left circumflex, *IMB* intermediate branch

the prediction model on the training set. This took into account of the clustering feature that each patient had multiple segments measured. Receiver-operating characteristic (ROC) curve with area under the curve (AUC) was used to access the performance of the prediction model. The derived prediction model was then validated by the test set.

Results

Baseline characteristics and angiographic findings (Table 2)

In the training set, 126/201 (62.7 %) patients had at least one ≥50 % stenosis (Table 2). A total of 3001 coronary segments were visualized angiographically. Of these, 136/3001 (4.5 %) were localized distally to occluded coronary segments and supplied by collateral pathways thus were excluded from the analysis. There remained 2865 coronary segments, of which 282/2865 (9.8 %) harboured ≥50 % stenoses. Among the lesions associated with ≥50 % stenosis, 89/282 (31.6 %) were in the RCA, 110/282 (39 %) in the LAD, 79/282 (29 %) in the LCx, and 4/282 (1.4 %) in the LM ($p < 0.001$).

Total calcium score and frequency of stenosis anywhere in the coronary tree (patient level)

In the training set, the median (interquartile range) total calcium score at patient level was 198.10 (10.65–557.40). The frequency of at least one coronary stenosis at the patient level increased proportionally with increasing total calcium score (p value <0.001). In patients with a total Agatston calcium score in the range 0–10, 5/50 (10 %)

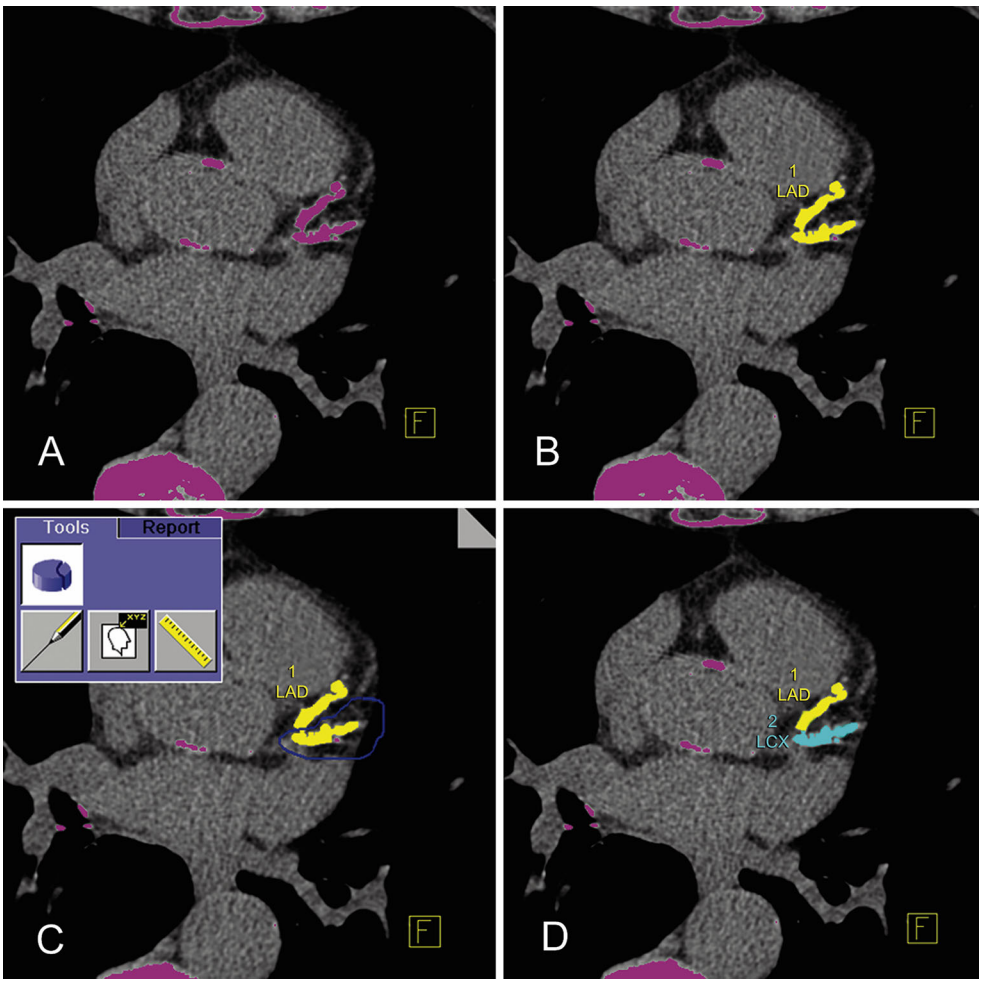

Fig. 2 Method for separation of connected calcifications in a slice. To assign calcifications to the corresponding individual coronary artery segment, there needed to be separation of connected lesions in a slice (**a**, **b**). To achieve this, calcifications were edited manually (**c**) and split (**d**) using the '3D Edit' function (C, *inset* and *arrow*) of the software (syngo Calcium Scoring). *LAD* left anterior descending artery, *LCx* left circumflex

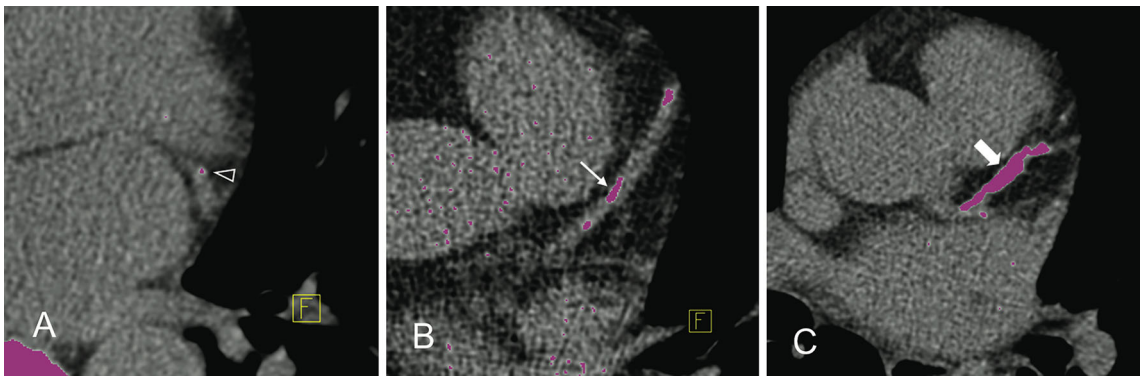

Fig. 3 Classification of calcification morphology. We applied a method validated by Kajinami et al. [14] for the classification of calcification morphology. Calcification morphology was classified visually as spotty (**a**, *arrowhead*), wide (**b**, *arrow*) and diffuse (**c**, *gross arrow*) based on the width and length of the calcification in relation to the coronary segment diameter (full description in Table 1)

patients had at least one significant stenosis. In patients with a total calcium score in the range 11–100, 20/32 (62.5 %) patients had at least one significant stenosis. In patients with a total calcium score in the range 101–400, 45/59 (76.3 %) patients had at least one significant stenosis. In patients with a total calcium score >400, 56/60

Table 1 Classification of calcification morphology on non-enhanced CT images. Modified from Kajinami et al. [14]

Calcification morphology	Lesion width[a]	Lesion length[b]
Diffuse	≥2/3 of coronary diameter	≥3/2 of coronary diameter
Wide	≥2/3 of coronary diameter or <2/3 of coronary diameter	<3/2 of coronary diameter or ≥3/2 of coronary diameter
Spotty	<2/3 of coronary diameter	<3/2 of coronary diameter
None	Undetectable	Undetectable

[a] Extent of calcification perpendicular to the longitudinal direction of the vessel

[b] Extent of lesion in the longitudinal direction of the vessel

(93.3 %) had at least one significant stenosis. The AUCs of total Agatston score for the detection of ≥50 % coronary stenosis at the patient level was 0.851 (CI 0.681–0.900). The OR for ≥50 % stenosis anywhere in the coronary tree (patient level) was approximately 1.9-fold greater ($p < 0.001$) for each unit of natural log of total calcium score (OR 1.908, CI 1.664–2.375).

Segmental calcium score (SCS)

In the training set, the range in SCS was 0–1370. The median (interquartile range) was 0 (0–6.65). There were 1735/2865 (60.6 %) segments which did not show any detectable calcification (SCS = 0). Of these, 68/1735 (3.9 %) harboured a ≥50 % stenosis.

Calcification morphology

In the training set, there were 431/2865 (15 %) spotty calcifications, 325/2865 (11.3 %) wide calcifications, and 374/2875 (13.1 %) diffuse calcifications.

Frequency of significant stenoses

The frequency of coronary stenosis increased proportionally with increasing SCS (Fig. 4, left column), and from spotty, to wide, to diffuse morphology (all p values <0.01). The frequency of significant stenoses associated with SCS and morphology in men and women according to age is given in Table 3. The AUCs for the detection of ≥50 % coronary stenosis were 0.739 (CI 0.706–0.771) for SCS, and 0.738 (CI 0.706–0.771) for calcification morphology (Fig. 4, right column).

Univariable analysis (Table 4)

The OR for ≥50 % stenosis was approximately 1.7-fold ($p = 0.005$) greater for patients with typical chest pain and 1.6-fold ($p = 0.023$) greater for patients with unstable angina or non-ST elevation myocardial infarction (acute coronary syndrome). For patients with dyslipidemia, the OR was increased 2.6-fold ($p < 0.001$), and for patients with a prior myocardial infarction the OR was increased 2.5-fold ($p < 0.001$). With distal segments as comparator, the OR for ≥50 % stenosis was approximately 1.6-fold ($p < 0.001$) greater for middle segments, and 1.8-fold ($p = 0.001$) greater for proximal segments. With the RCA as comparator, the OR was approximately 0.7-fold ($p = 0.039$) smaller for the LCx, and 0.2-fold ($p < 0.001$) smaller for the LM; the OR's for the RCA and LAD were similar. For each unit of natural log of SCS, the OR of ≥50 % stenosis was 1.5-fold ($p < 0.001$) greater. The presence of spotty calcifications had an OR for stenosis approximately 2.7-fold ($p < 0.001$) greater than the absence of calcification, wide calcifications approximately 4.3-fold ($p < 0.001$) greater, and diffuse calcifications approximately 9.1-fold ($p < 0.001$) greater than the absence of calcification.

Multivariable analysis (Table 5)

In a GEE model, the OR for coronary stenosis was approximately 1.8-fold greater ($p = 0.006$) in patients with typical chest pain, twofold ($p = 0.014$) greater in patients with acute coronary syndrome, and twofold greater ($p < 0.001$) in patients with prior myocardial infarction. The presence of spotty calcifications had an OR for stenosis approximately 2.3-fold ($p < 0.001$) greater than the absence of calcification, wide calcifications approximately 2.7-fold ($p < 0.001$) greater, and diffuse calcifications approximately 4.6-fold ($p < 0.001$) greater than the absence of calcification. With distal segments as comparator, each unit of natural log of SCS in middle segments corresponded to an OR approximately 1.2-fold ($p < 0.001$) greater; in proximal segments this corresponded to an OR 1.1-fold greater ($p = 0.021$). The LM coronary artery had an OR for stenosis approximately 0.2-fold ($p = 0.001$) smaller than the RCA, whereas the remaining coronary vessels were similar.

Prediction score

Based on the coefficients (multiplied by 100) of the final GEE model (Table 5), a score for the prediction of the probability of ≥50 % stenosis in a given segment (*P-score*) was calculated as follows:

Table 2 Baseline characteristics

Characteristic	Training sample	Test sample	*p* value[e]
No. of patients	201	201	–
Age			
Mean age (sd)[a] (years)	59 (12)	60 (10)	0.52[f]
Age range	21–87	35–80	–
Age groups: no. (%)	–	–	0.81
≤50	38/201 (19 %)	33/201 (17 %)	–
51–60	79/201 (39 %)	80/201 (40 %)	–
61–70	50/201 (25 %)	57/201 (28 %)	–
>70	34/201 (17 %)	31/201 (15 %)	–
Men/women: no. (%)	142 (71 %)/59 (29 %)	137 (68 %)/64 (32 %)	0.59
Patient clinical presentation: no. (%)			
Typical chest pain[b]	97/201 (48 %)	57/201 (28 %)	<0.001
Atypical chest pain[c]	71/201 (35 %)	76/201 (38 %)	0.61
Acute coronary syndrome[d]	33/201 (17 %)	68/201 (34 %)	<0.001
Cardiovascular risk factors: no. (%)			
Obesity (Body Mass Index ≥30 kg/m^2)	48/201 (24 %)	50/201 (25 %)	0.84
Smoking (current or past)	63/201 (31 %)	66/201 (33 %)	0.75
Hypertension (blood pressure ≥140/90 mmHg, or on anti-hypertension medication)	106/201 (53 %)	110/201 (55 %)	0.69
Dyslipidemia (serum cholesterol >200 mg/dL or 5.18 mmol/L)	136/201 (68 %)	100/201 (50 %)	<0.001
Diabetes mellitus (plasma glucose ≥126 mg/dL or 7.0 mmol/L)	25/201 (12 %)	26/201 (13 %)	0.88
Family history [presence of CAD in a first-degree female (<65 years) or male (<55 years) relative]	90/201 (45 %)	106/201 (53 %)	0.11
Prior myocardial infarction	43/201 (21 %)	21/201 (11 %)	0.003
Medication before CT and heart rate			
Beta-blockers: no. (%)	142/201 (71 %)	135/201 (67 %)	0.11
Mean heart rate during scan (sd)[a] (beats/min)	58 (11)	60 (8)	0.77
Total calcium score (Agatston; patient level)			
Range	0–3839	0–3394	–
Mean (sd)[a]	450.37 (661.23)	346.60 (492.02)	0.70[f]
Median (IQ)[g]	198.10 (10.65–557.40)	214.70 (14.70–443.80)	1.00[h]
Calcium score groups: no. (%)	–	–	0.79
0–10	50/201 (25 %)	47/201 (23 %)	–
11–100	32/201 (16 %)	32/201 (16 %)	–
101–400	59/201 (29 %)	68/201 (34 %)	–
>400	60/201 (30 %)	54/201 (27 %)	–

[a] Standard deviation; [b] retrosternal pain occurring with exercise, relieved by rest and by administration of nitrates; [c] any 2 or 1 features of typical chest pain; [d] unstable angina or non-ST elevation myocardial infarction; [e] Chi squared test unless otherwise specified; [f] Mann–Whitney U test; [g] interquartile range; [h] independent samples median test

$$\begin{aligned} \textit{P-score} = {} & 12 \times \ln(\text{SCS})(\text{if proximal}) + 17 \\ & \times \ln(\text{SCS})(\text{if middle}) + 83(\text{if spotty}) \\ & + 99(\text{if wide}) + 153(\text{if diffuse}) \\ & + 56(\text{if typical chest pain}) \\ & + 69(\text{if acute coronary syndrome}) \\ & + 68(\text{if prior myocardial infarction}) \\ & - 178(\text{if LM}) - 362 \end{aligned}$$

The probability of ≥50 % coronary stenosis increased with the extent (i.e., SCS, morphology) of coronary calcification. This probability was related to the *P-score* through the following equation:

$$\text{Probability}(\geq 50\,\%\,\text{stenosis}) = 1/[1 + \exp(-\textit{P-score})]$$

Training set and test set (Fig. 5)

The prediction model showed a good diagnostic performance when validated in the test set. The AUC in the test set was 0.786 (CI 0.757–0.814). This value was similar to

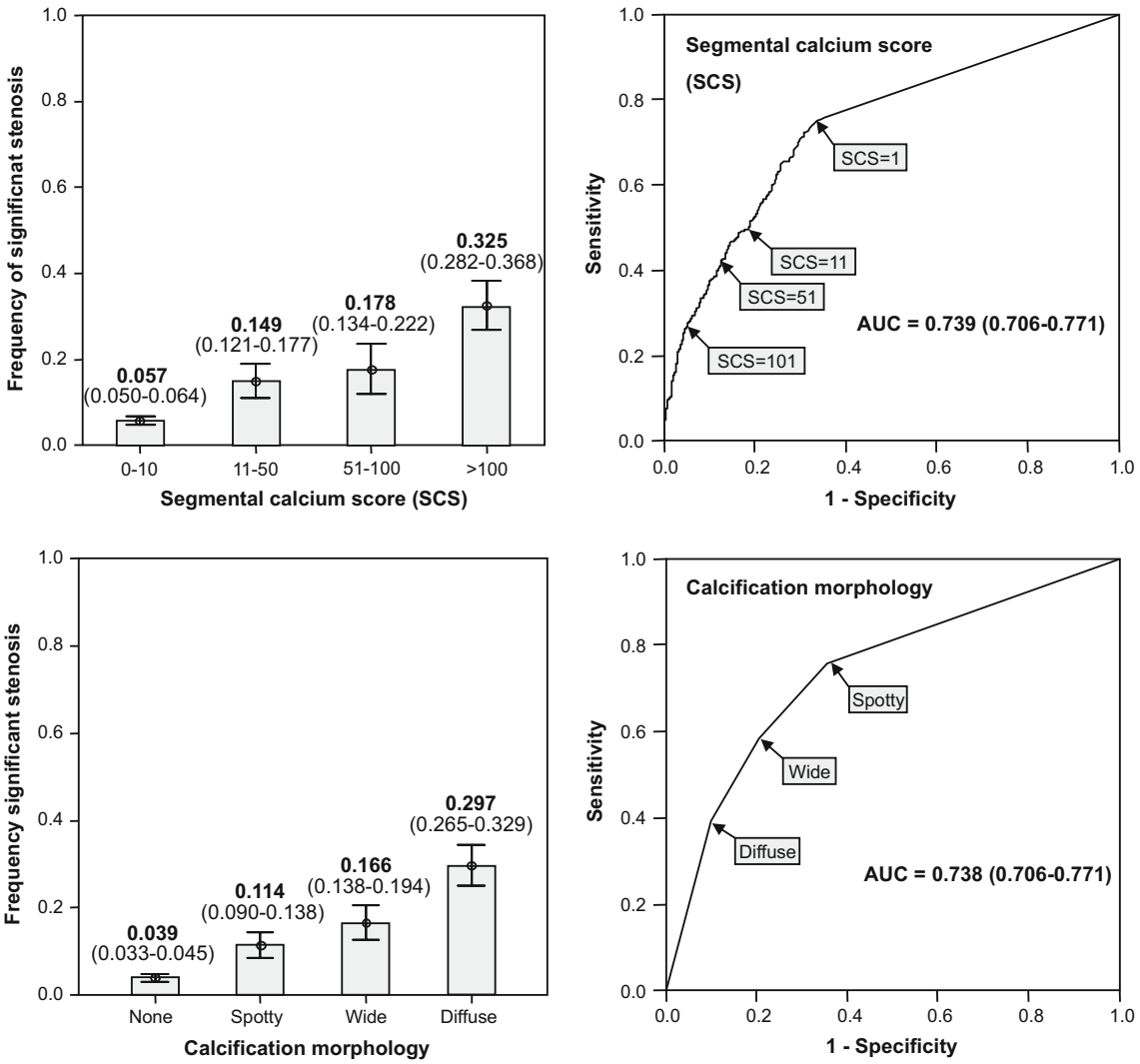

Fig. 4 Segmental calcium score (SCS) and calcification morphology: frequency of associated significant stenoses (*left column*) and ROC curves (*right column*). The frequency of coronary stenosis (*left column*) increased proportionally with increasing SCS. The frequency of stenosis also increased from spotty, to wide, to diffuse morphology. The diagnostic performances of SCS and morphology in the detection of ≥50 % stenosis (*right column*) were similar. *Arrows* and *labels* indicate different calcification thresholds for positivity (i.e., ≥50 % coronary artery stenosis)

the AUC in the training set that was 0.795 (CI 0.770–0.819) showing a consistent performance. The Youden's index in the training set gave an optimal probability threshold equal to or greater than 9.2 %, which yielded sensitivity and specificity of 0.752 and 0.712, respectively. In the test set, the optimal probability threshold was equal to or greater than 6.8 %, which yielded sensitivity and specificity of 0.748 and 0.689, respectively.

Discussion

Summary of findings

The probability of ≥50 % diameter stenosis increased with SCS, and from the spotty, to the wide, to the diffuse calcification morphology (Fig. 4, left column), in keeping with findings by Lau et al. [16] and Kajinami et al. [14]. For both SCS and calcification morphology the use of a high-specificity

Table 3 Frequency of significant stenoses in relation to SCS ranges and morphology (in men and women according to age)

	SCS					Calcification morphology				
	0–10	11–50	51–100	>100	*p* value*	None	Spotty	Wide	Diffuse	*p* value*
Men										
≤50	16/384	2/17	0/2	¼	0.114	11/328	5/58	1/13	2/8	**0.012**
	(4.2 %)	(11.8 %)	(0 %)	(25 %)		(3.4 %)	(8.6 %)	(7.7 %)	(25 %)	
51–60	43/623	20/11	12/63	25/71	**<0.001**	20/495	20/140	20/113	40/120	**<0.001**
	(6.9 %)	(18 %)	(19 %)	(35.2 %)		(4 %)	(14.3 %)	(17.7 %)	(33.3 %)	
61–70	13/260	6/59	9/35	26/89	**<0.001**	7/198	5/63	14/70	28/112	**<0.001**
	(5 %)	(10.2 %)	(25.7 %)	(29.2 %)		(3.5 %)	(7.9 %)	(20 %)	(25 %)	
>70	20/162	8/39	4/36	15/49	**0.016**	12/117	7/48	8/57	20/64	**0.003**
	(12.3 %)	(20.5 %)	(11.1 %)	(30.6 %)		(10.3 %)	(14.6 %)	(14 %)	(31.3 %)	
Women										
≤50	4/139	0/6	0/2	Value not observed	0.888	3/130	1/13	0/3	0/1	0.703
	(2.9 %)	(0 %)	(0 %)			(2.3 %)	(7.7 %)	(0 %)	(0 %)	
51–60	3/234	0/10	2/99	3/4	**<0.001**	3/211	0/24	2/11	3/11	**<0.001**
	(1.3 %)	(0 %)	(22.2 %)	(75 %)		(1.4 %)	(0 %)	(18.2 %)	(27.3 %)	
61–70	16/209	7/39	1/14	5/14	**0.003**	8/170	6/48	5/31	10/27	**<0.001**
	(7.7 %)	(17.9 %)	(7.1 %)	(35.7 %)		(4.7 %)	(12.5 %)	(16.1 %)	(37 %)	
>70	7/114	4/35	2/8	8/24	**0.001**	4/86	5/37	4/27	8/31	**0.014**
	(6.1 %)	(11.4 %)	(25 %)	(33.3 %)		(4.7 %)	(13.5 %)	(14.8 %)	(25.8 %)	

* Chi square test. Significant *p* values are bolded

threshold was associated with a much lower sensitivity, and a high-sensitivity threshold was associated with a much lower specificity (Fig. 4, right column), implying that SCS and calcification morphology if used *per se* were rather crude predictors of ≥50 % stenosis. The compensatory enlargement of atherosclerotic coronary arteries (positive vessel wall remodeling) may explain this finding [17]. By combining patient's symptoms, clinical history and lesion location within the coronary tree, the predictive value of SCS and calcification morphology could be improved. We developed a multivariable prediction model based on SCS, calcification morphology, the patient's symptoms and clinical history to predict the probability of ≥50 % diameter stenosis in the same coronary segment. The prediction model was tested in a test sample not used for the development of the formula and revealed consistent performance.

Clinical implications

The total Agatston calcium score is a sensitive predictor of coronary stenosis anywhere in the coronary tree when a low positivity cut-off is used (94 % sensitivity with a cut-off of Agatston score greater than 0), but with a poor specificity (47 % specificity) [2]. On the other hand, if a higher cut-off is chosen, coronary calcium has better specificity at the expense of sensitivity.

There is a weak relationship between intermediate calcium scores (e.g., between 100 and 399) and associated stenosis. CCTA can partly overcome this weakness [18]. The interpretation of CCTA however can be challenged by focal bulky calcifications. Bulky calcifications can be expected in 10 % of coronary segments in patients with intermediate pre-test likelihood of coronary artery disease, and of these one in four are associated with significant stenoses [19]. Bulky calcifications typically lead to overestimation of lesion severity (false positive diagnosis) [19–22] related to limited spatial resolution of CCTA and the resulting visual impression known as the 'blooming effect'. Whether focal segmental calcifications can help predict the probability of underlying coronary stenosis was the research question addressed by this study.

The formula described here may help estimate the probability of significant stenosis in the context of reading CCTA in a patient with focal bulky calcifications. Whether or not further action should be taken—either ordering a further diagnostic test or initiating aggressive medical therapy—will not depend exclusively on the result of the prediction model, but rather on the global patient assessment. For instance, in a patient with suspected high-risk coronary artery disease (defined as 2-vessel disease involving the LAD, 3-vessel disease or involvement of the LM) further testing and intention to treat may be the first option, as these patients are likely to benefit from revascularization [23, 24]. On the other hand, in a patient with low-risk coronary artery disease (e.g., 1-vessel disease involving a non-prognostic vessel) aggressive medical treatment may be the first option.

Table 4 Univariable logistic regression models for the prediction of angiographically proven significant coronary stenosis

Characteristic	Odds ratio (95 % CI)	*p* value*
Age	1.032 (1.015–1.0494)	**<0.001**
Gender (male)	1.629 (1.086–2.445)	**0.018**
Typical chest pain	1.694 (1.178–2.438)	**0.005**
Atypical chest pain	0.340 (0.214–0.538)	**<0.001**
Acute coronary syndrome	1.625 (1.068–2.472)	**0.023**
Obesity	0.986 (0.679–1.432)	0.941
Smoking	1.069 (0.755–1.513)	0.708
Hypertension	1.098 (0.763–1.579)	0.615
Dyslipidemia	2.606 (1.523–4.459)	**<0.001**
Diabetes	0.819 (0.513–1.307)	0.402
Family history of CAD	0.781 (0.550–1.108)	0.166
Prior myocardial infarction	2.537 (1.776–3.623)	**<0.001**
Segment location**		
Distal and side branches	Odds ratio comparator	
Middle	2.545 (1.913–3.386)	**<0.001**
Proximal	1.777 (1.272–2.483)	**0.001**
Vessel		
RCA	Odds ratio comparator	
LAD	0.995 (0.718–1.379)	0.976
LCx	0.722 (0.529–0.984)	**0.039**
LM	0.150 (0.054–0.416)	**<0.001**
SCS (ln)	1.500 (1.399–1.604)	**<0.001**
Calcification morphology		
Spotty	2.732 (1.898–3.934)	**<0.001**
Wide	4.269 (2.836–6.427)	**<0.001**
Diffuse	9.144 (6.297–13.277)	**<0.001**

* Significant *p* values are bolded

** Proximal segments included segments 1, 5, 6, and 11. Middle segments included segments 2, 3, 7, and 13. Distal and side branches included segments 4a, 4b, 8, 9, 10, 12, 14, 15, and 16 (9, 15)

The diagnostic performance of the prediction model in the test sample (AUC = 0.786) was worse than that of patient-level Agatston calcium score (AUC = 0.851). However, a direct comparison does not make sense because the total Agatston score is predictive of stenosis anywhere in the coronary tree at the patient level, whereas the rationale of this prediction model is at segmental or lesion level, not at the patient level. The prediction model may help in a subset of patients with intermediate total Agatston calcium scores (100–399) and one or two bulky calcified plaques that challenge CCTA interpretation.

Sharp reconstruction kernels partially compensate for the blooming effect, however this comes at the expense of increased image noise. Deconvolution filters require long computational times and have not been validated in clinical practice [25]. Dual-energy scan techniques allow the acquisition of separate low- and high-energy images which are then synthesized to cancel high-density structures such as calcifications [26, 27]. Compared to the conventional (single-energy) scan technique, these approaches are characterised by roughly double temporal resolution or spatial resolution, hence the added value for coronary artery imaging in patients remains uncertain. The possibility of obtaining virtual non-contrast images from a single contrast-enhanced CCTA [28] may obviate the need to perform a non-enhanced scan prior to CCTA. Iterative reconstruction algorithms can reduce radiation exposure to patients without decreasing overall image quality in coronary calcium scoring [29] and CCTA [30], however their effect on the diagnostic performance of CCTA in severely calcified coronary arteries has not been firmly established.

Limitations

The Agatston calcium score is not a physical measurement of calcification [11]. There was however a very high correlation between the Agatston and the volume/mass scores. SCS does not include non-calcified plaque. The training set and test set included two groups of consecutive patients. Small differences between groups may explain the slightly poorer fitting of the model on the test set compared to the training set. The test set had less patients with typical chest pain and more patients with atypical chest pain. The test set may thus represent a slightly more challenging patient group. The reported results are therefore a conservative estimate of the prediction model's performance. Further research may be warranted to define in which patient population the analysis of SCS additional to CCTA may be most beneficial to improve diagnostic performance.

Future developments

The semi-automated quantification of coronary plaque burden and components (calcified and non-calcified) may represent a more accurate approach for the characterisation of coronary artery plaques [31–34]. These methods however require time-intensive manual input, as opposed to the quick method described here. The feasibility of stress myocardial CT perfusion imaging has been demonstrated recently [35–40] as capable of adding functional information on the haemodynamic significance of coronary stenoses. However, CT perfusion imaging requires additional patient radiation exposure, contrast administration and the administration of a pharmacological stress agent. The possibility of a CT-derived fractional flow reserve measurement based on computational fluid dynamics modelling, albeit computationally difficult and time-consuming, has also been shown with very promising results [41]. The utility of computational FFR in very

Table 5 GEE logistic regression (final) model for the prediction of angiographically proven significant coronary stenosis

Model*	Odds ratio (95 % CI)	*p* value**	Coefficient
Clinical presentation			
Typical chest pain	1.755 (1.175–2.622)	**0.006**	0.562
Acute coronary syndrome	1.989 (1.151–3.439)	**0.014**	0.688
Risk factors			
Prior myocardial infarction	1.982 (1.397–2.812)	**<0.001**	0.684
Vessel			
LM	0.169 (0.059–0.482)	**0.001**	−1.776
Calcification morphology			
Spotty	2.303 (1.567–3.384)	**<0.001**	0.834
Wide	2.690 (1.698–4.260)	**<0.001**	0.989
Diffuse	4.614 (2.842–7.491)	**<0.001**	1.529
SCS (ln)			
If middle segment	1.189 (1.084–1.304)	**<0.001**	0.173
If proximal segment	1.125 (1.018–1.242)	**0.021**	0.117

* The model Wald Chi square was 226.32 ($p < 0.001$)

** Only variables that retained significant p values in the multivariable model are reported here. Age, gender, atypical chest pain, dyslipidemia and LCx vessel location had significant p values at univariable analysis, but not at multivariable analysis

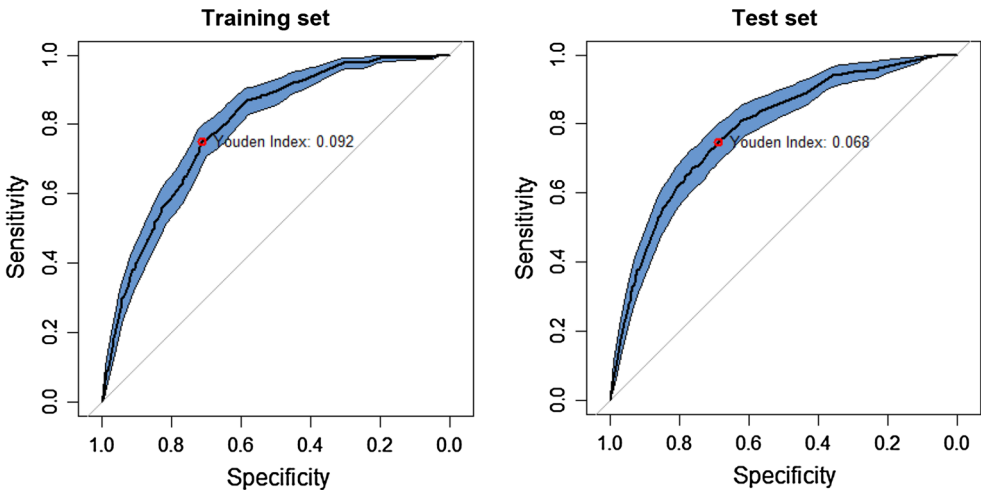

Fig. 5 Performance of the multivariable model (ROC curves) in the training set and test set. The Youden's index in the training set gave an optimal probability threshold equal to or greater than 9.2 %, which yielded sensitivity and specificity of 0.752 and 0.712, respectively. In the test set, the optimal probability threshold was equal to or greater than 6.8 %, which yielded sensitivity and specificity of 0.748 and 0.689, respectively

heavily calcified coronary vessels, however, remains uncertain.

Acknowledgments This work forms part of the translational research portfolio of the NIHR Cardiovascular Biomedical Research Unit at Barts, which is supported and funded by the NIHR.

Compliance with ethical standards

Conflict of interest None declared.

References

1. Bielak LF, Rumberger JA, Sheedy PF II et al (2000) Probabilistic model for prediction of angiographically defined obstructive coronary artery disease using electron beam computed tomography calcium score strata. Circulation 102(4):380–385
2. Breen JF, Sheedy PF II, Schwartz RS et al (1992) Coronary artery calcification detected with ultrafast CT as an indication of coronary artery disease. Radiology 185(2):435–439
3. Budoff MJ, Diamond GA, Raggi P et al (2002) Continuous probabilistic prediction of angiographically significant coronary artery disease using electron beam tomography. Circulation 105(15):1791–1796
4. Haberl R, Becker A, Leber A et al (2001) Correlation of coronary calcification and angiographically documented stenoses in patients with suspected coronary artery disease: results of 1764 patients. J Am Coll Cardiol 37(2):451–457
5. Meijboom WB, van Mieghem CA, Mollet NR et al (2007) 64-Slice computed tomography coronary angiography in patients with high, intermediate, or low pretest probability of significant coronary artery disease. J Am Coll Cardiol 50(15):1469–1475
6. Meijboom WB, Weustink AC, Pugliese F et al (2007) Comparison of diagnostic accuracy of 64-slice computed tomography

coronary angiography in women versus men with angina pectoris. Am J Cardiol 100(10):1532–1537
7. Mollet NR, Cademartiri F, van Mieghem CA et al (2005) High-resolution spiral computed tomography coronary angiography in patients referred for diagnostic conventional coronary angiography. Circulation 112(15):2318–2323
8. Hausleiter J, Meyer T, Hermann F et al (2009) Estimated radiation dose associated with cardiac CT angiography. JAMA 301(5):500–507
9. Austen WG, Edwards JE, Frye RL et al (1975) A reporting system on patients evaluated for coronary artery disease. Report of the Ad Hoc Committee for Grading of Coronary Artery Disease, Council on Cardiovascular Surgery, American Heart Association. Circulation 51(4 Suppl):5–40
10. Mark DB, Berman DS, Budoff MJ et al (2010) ACCF/ACR/AHA/NASCI/SAIP/SCAI/SCCT 2010 expert consensus document on coronary computed tomographic angiography: a report of the American College of Cardiology Foundation Task Force on Expert Consensus Documents. J Am Coll Cardiol 55(23):2663–2699
11. Agatston AS, Janowitz WR, Hildner FJ et al (1990) Quantification of coronary artery calcium using ultrafast computed tomography. J Am Coll Cardiol 15(4):827–832
12. Callister TQ, Cooil B, Raya SP et al (1998) Coronary artery disease: improved reproducibility of calcium scoring with an electron-beam CT volumetric method. Radiology 208(3):807–814
13. McCollough CH, Ulzheimer S, Halliburton SS et al (2007) Coronary artery calcium: a multi-institutional, multimanufacturer international standard for quantification at cardiac CT. Radiology 243(2):527–538
14. Kajinami K, Seki H, Takekoshi N, Mabuchi H (1997) Coronary calcification and coronary atherosclerosis: site by site comparative morphologic study of electron beam computed tomography and coronary angiography. J Am Coll Cardiol 29(7):1549–1556
15. Pugliese F, Mollet NR, Hunink MG et al (2008) Diagnostic performance of coronary CT angiography by using different generations of multisection scanners: single-center experience. Radiology 246(2):384–393
16. Lau GT, Ridley LJ, Schieb MC et al (2005) Coronary artery stenoses: detection with calcium scoring, CT angiography, and both methods combined. Radiology 235(2):415–422
17. Glagov S, Weisenberg E, Zarins CK et al (1987) Compensatory enlargement of human atherosclerotic coronary arteries. N Engl J Med 316(22):1371–1375
18. Hadamitzky M, Distler R, Meyer T et al (2011) Prognostic value of coronary computed tomographic angiography in comparison with calcium scoring and clinical risk scores. Circ Cardiovasc Imaging 4(1):16–23
19. Meijboom WB, Meijs MF, Schuijf JD et al (2008) Diagnostic accuracy of 64-slice computed tomography coronary angiography: a prospective, multicenter, multivendor study. J Am Coll Cardiol 52(25):2135–2144
20. Abdulla J, Pedersen KS, Budoff M, Kofoed KF (2012) Influence of coronary calcification on the diagnostic accuracy of 64-slice computed tomography coronary angiography: a systematic review and meta-analysis. Int J Cardiovasc Imaging 28(4):943–953
21. Alkadhi H, Scheffel H, Desbiolles L et al (2008) Dual-source computed tomography coronary angiography: influence of obesity, calcium load, and heart rate on diagnostic accuracy. Eur Heart J 29(6):766–776
22. Yan RT, Miller JM, Rochitte CE et al (2013) Predictors of inaccurate coronary arterial stenosis assessment by CT angiography. JACC Cardiovasc Imaging 6(9):963–972
23. de Feyter PJ, Nieman K (2012) CCTA to guide revascularization for high-risk CAD: a 'cliff hanger'. Eur Heart J 33(24):3011–3013
24. Min JK, Berman DS, Dunning A et al (2012) All-cause mortality benefit of coronary revascularization vs. medical therapy in patients without known coronary artery disease undergoing coronary computed tomographic angiography: results from CONFIRM (COronary CT Angiography EvaluatioN For Clinical Outcomes: An InteRnational Multicenter Registry). Eur Heart J 33(24):3088–3097
25. Rollano-Hijarrubia E, Niessen W, Weinans H et al (2007) Histogram-based selective deblurring to improve computed tomography imaging of calcifications. Invest Radiol 42(1):8–22
26. Johnson TR, Krauss B, Sedlmair M et al (2007) Material differentiation by dual energy CT: initial experience. Eur Radiol 17(6):1510–1517
27. Schwarz F, Nance JW Jr, Ruzsics B et al (2012) Quantification of coronary artery calcium on the basis of dual-energy coronary CT angiography. Radiology 264(3):700–707
28. Bischoff B, Kantert C, Meyer T et al (2012) Cardiovascular risk assessment based on the quantification of coronary calcium in contrast-enhanced coronary computed tomography angiography. Eur Heart J Cardiovasc Imaging 13(6):468–475
29. Schindler A, Vliegenthart R, Schoepf UJ et al (2014) Iterative image reconstruction techniques for CT coronary artery calcium quantification: comparison with traditional filtered back projection in vitro and in vivo. Radiology 270(2):387–393
30. Gosling O, Loader R, Venables P et al (2010) A comparison of radiation doses between state-of-the-art multislice CT coronary angiography with iterative reconstruction, multislice CT coronary angiography with standard filtered back-projection and invasive diagnostic coronary angiography. Heart 96(12):922–926
31. Dey D, Schepis T, Marwan M et al (2010) Automated three-dimensional quantification of noncalcified coronary plaque from coronary CT angiography: comparison with intravascular US. Radiology 257(2):516–522
32. Leber AW, Becker A, Knez A et al (2006) Accuracy of 64-slice computed tomography to classify and quantify plaque volumes in the proximal coronary system: a comparative study using intravascular ultrasound. J Am Coll Cardiol 47(3):672–677
33. Schepis T, Marwan M, Pflederer T et al (2010) Quantification of non-calcified coronary atherosclerotic plaques with dual-source computed tomography: comparison with intravascular ultrasound. Heart 96(8):610–615
34. Sun J, Zhang Z, Lu B et al (2008) Identification and quantification of coronary atherosclerotic plaques: a comparison of 64-MDCT and intravascular ultrasound. AJR Am J Roentgenol 190(3):748–754
35. Bamberg F, Becker A, Schwarz F et al (2011) Detection of hemodynamically significant coronary artery stenosis: incremental diagnostic value of dynamic CT-based myocardial perfusion imaging. Radiology 260(3):689–698
36. Bamberg F, Hinkel R, Schwarz F et al (2012) Accuracy of dynamic computed tomography adenosine stress myocardial perfusion imaging in estimating myocardial blood flow at various degrees of coronary artery stenosis using a porcine animal model. Invest Radiol 47(1):71–77
37. Ho KT, Chua KC, Klotz E, Panknin C (2010) Stress and rest dynamic myocardial perfusion imaging by evaluation of complete time-attenuation curves with dual-source CT. JACC Cardiovasc Imaging 3(8):811–820
38. Rochitte CE, George RT, Chen MY et al (2014) Computed tomography angiography and perfusion to assess coronary artery stenosis causing perfusion defects by single photon emission computed tomography: the CORE320 study. Eur Heart J 35(17):1120–1130

39. Rossi A, Dharampal A, Wragg A et al (2014) Diagnostic performance of hyperaemic myocardial blood flow index obtained by dynamic computed tomography: Does it predict functionally significant coronary lesions? Eur Heart J Cardiovasc Imaging 15(1):85–94
40. Rossi A, Uitterdijk A, Dijkshoorn M et al (2013) Quantification of myocardial blood flow by adenosine-stress CT perfusion imaging in pigs during various degrees of stenosis correlates well with coronary artery blood flow and fractional flow reserve. Eur Heart J Cardiovasc Imaging 14(4):331–338
41. Norgaard BL, Leipsic J, Gaur S et al (2014) Diagnostic performance of noninvasive fractional flow reserve derived from coronary computed tomography angiography in suspected coronary artery disease: the NXT trial (analysis of coronary blood flow using CT angiography: next steps). J Am Coll Cardiol 63(12):1145–1155
42. Budoff MJ, Achenbach S, Blumenthal RS et al (2006) Assessment of coronary artery disease by cardiac computed tomography: a scientific statement from the American Heart Association Committee on Cardiovascular Imaging and Intervention, Council on Cardiovascular Radiology and Intervention, and Committee on Cardiac Imaging, Council on Clinical Cardiology. Circulation 114(16):1761–1791